

Modern NN Force Predictions for the Total ND Cross Section up to 300 MeV

H. Witała*, H. Kamada†, A. Nogga , W. Glöckle

Institute for Theoretical Physics II, Ruhr-University Bochum, D-44780 Bochum, Germany.

Ch. Elster

*Institute of Nuclear and Particle Physics, and Department of Physics,
Ohio University, Athens, OH 45701*

D. Hüber

Los Alamos National Laboratory, M.S.B283, Los Alamos, NM 87544

(March 23, 2022)

Abstract

For several modern nucleon-nucleon potentials state-of-the-art Faddeev calculations are carried out for the nd total cross section between 10 and 300 MeV projectile energy and compared to new high precision measurements. The agreement between theory and data is rather good, with exception at the higher energies where a 10% discrepancy builds up. In addition the convergence of the multiple scattering series incorporated in the Faddeev scheme is studied numerically with the result, that rescattering corrections remain important. Based on this multiple scattering series the high energy limit of the total nd cross section is also investigated analytically. In contrast to the naive expectation that the total nd cross section is the sum of the np and nn total cross sections we find additional effects resulting from the rescattering processes, which have different signs and different behavior as function of the energy. A shadowing effect in the high energy limit only occurs for energies higher than 300 MeV. The expressions in the high energy limit have qualitatively a similar behavior as the exactly calculated expressions, but can be expected to be valid quantitatively only at much higher energies.

*Permanent address: Institute of Physics, Jagellonian University, PL-30059 Cracow, Poland

†Present address: Institut für Strahlen und Kernphysik der Universität Bonn, Nussallee 14-16, D-53115 Bonn, Germany

PACS: 28.20.Cz, 21.45+v,25.10+s

Typeset using REVTeX

I. INTRODUCTION

For three-nucleon scattering the total neutron-deuteron (nd) cross section is the simplest observable, since it is integrated over the angular distribution in elastic nd scattering and all the angular and continuous energy distributions of the three-nucleon (3N) breakup process. If the theory does not agree with experiment, one has to expect that for some individual observables even stronger discrepancies might exist. On the other hand if there is agreement, possible discrepancies in some individual unpolarized differential cross sections have at least to average out. It is the aim of this article to compare precise new data between 10 and 300 MeV neutron laboratory energy for the total nd cross section [1] with fully converged Faddeev calculations based on the most modern nucleon-nucleon (NN) forces. The calculations are based on a strictly nonrelativistic treatment. Despite of this apparent restriction, we think that this comparison of theory and experiment will be an important benchmark result.

A first presentation of our results appeared in [1]. Here we want to give a more detailed description and explicitly show that our theoretical results are stable under the exchange of one of the most modern NN potentials by another one. Detailed studies on the size of the contributions of the first few terms in the multiple scattering expansion to the total nd cross section are given.

In order to obtain more insight into the behavior of the multiple scattering series for the total nd cross section we provide analytical high energy expansions for the first few terms. Compared to the most naive picture, which in the high energy limit would equate the total nd cross section with the sum of the total cross sections for neutron-proton (np) and neutron-neutron (nn) scattering, the rigorously calculated result is smaller for energies up to 300 MeV. Obviously shadowing effects can be expected. However, rescattering processes may *a priori* also enhance the total nd cross section. It is shown that rescattering processes of second order in the NN t-matrix lead to shadowing and antishadowing effects. In principle these features are known for the 3N scattering amplitude from studies in the framework of Glauber theory [2–5]. In contrast to this formulation we start from a multiple scattering series, which implies that it is an ordering according to powers of the NN t-matrix. The analytical steps leading to the high energy limit of the first leading terms are carried out in well defined integrals. There are no *a priori* assumptions involved about the scattering process, such as, e.g. diffraction type approximations. We observe that in the high energy limit a shadowing effect only occurs for energies larger than 300 MeV, below this energy the contributions second order in the NN t-matrix in the high energy limit enhance the sum of np and nn total cross sections. Furthermore, it is interesting to see that even at 300 MeV the high energy limit is quantitatively not yet reached. Nevertheless, the analytical studies make the underlying physics more transparent. An analogous investigation for the much simpler case of 3 bosons was performed in Ref. [6].

The paper is organized as follows. In Sec. II we briefly describe the Faddeev framework, its multiple scattering expansion, the leading order terms in the NN t-matrix for obtaining the nd total cross section, and the high energy limit of the corresponding expressions. The derivation of the high energy limit is explicitly given in Appendices A and B. In Sec. III we present the results of our exact Faddeev calculations in comparison with the data and with the calculations in the high energy limit. In Sec. IV we study the effect of three-nucleon forces (3NF) on the total nd cross section. In addition, a simple estimate of relativistic

kinematic effects is given. We conclude in Sec. V.

II. LEADING MULTIPLE SCATTERING TERMS FOR THE ND TOTAL CROSS SECTION AND HIGH ENERGY LIMIT

We solve the Faddeev equations for 3N scattering in the form

$$T|\Phi\rangle = tP|\Phi\rangle + tPG_0T|\Phi\rangle, \quad (2.1)$$

where t is the NN t-matrix, the operator P the sum of a cyclical and an anticyclical permutation of 3 objects and $|\Phi\rangle$ the initial channel state composed of a deuteron and the momentum eigenstate of the projectile nucleon. The full breakup operator is

$$U_0 = (1 + P)T, \quad (2.2)$$

defining the physical meaning of the T -operator. The iteration of Eq. (2.1) together with Eq. (2.2) generates the multiple scattering series for the breakup process.

Furthermore, the operator for elastic nd scattering is given by

$$U = PG_0^{-1} + PT. \quad (2.3)$$

Our aim is the evaluation and the understanding of the total nd cross section, which is given via the optical theorem

$$\sigma_{tot}^{nd} = -(2\pi)^3 \frac{4m}{3q_0} \text{Im}\langle\Phi|U|\Phi\rangle. \quad (2.4)$$

Here m is the nucleon mass and q_0 is the asymptotic momentum of the projectile nucleon relative to the deuteron. Thus solving Eq. (2.1) and using Eq. (2.3) yields the desired result in the form Eq. (2.4).

In order to achieve insight how the total nd cross section is formed at high energies we consider the multiple scattering expansion of the operator U as given in Eq. (2.3). The first few terms constitute a power series expansion in the NN t-matrix

$$U = PG_0^{-1} + PtP + PtG_0PtP + \dots \quad (2.5)$$

At higher energies only a few terms in this expansion may be sufficient to describe the total nd cross section. We evaluate the different terms in the series numerically and study their contributions to the total cross section in Sec. III.

In order to obtain analytical insight into the contributions to the total cross section we consider the imaginary part of the operator U as given in Eq. (2.5) between the channel states $|\Phi\rangle$ and obtain

$$\begin{aligned} 2i \text{Im}\langle\Phi|U|\Phi\rangle &= \langle\Phi|U|\Phi\rangle - \langle\Phi|U|\Phi\rangle^* \\ &= \langle\Phi|P(t - t^\dagger)P|\Phi\rangle + \langle\Phi|PtG_0PtP - Pt^\dagger G_0^* Pt^\dagger P|\Phi\rangle + \dots \end{aligned} \quad (2.6)$$

Since the first term in Eq. (2.5) is real, it does not contribute to the total cross section. The second order term in the NN t-matrix can be rewritten as

$$\begin{aligned} \langle \Phi | PtG_0PtP - Pt^\dagger G_0^* Pt^\dagger P | \Phi \rangle &= \langle \Phi | P(t - t^\dagger) PG_0 t P | \Phi \rangle \\ &\quad - \langle \Phi | P(t - t^\dagger) PG_0 t P | \Phi \rangle^* + \langle \Phi | Pt^\dagger P (G_0 - G_0^*) t P | \Phi \rangle, \end{aligned} \quad (2.7)$$

which will be the starting point for extracting the high energy limit analytically.

Let us first concentrate on the first order term of Eq. (2.6) and work out the permutations. For the channel state $|\Phi\rangle$ we choose

$$|\Phi\rangle = |\Phi\rangle_1 \equiv |\varphi_d\rangle_{23} |\mathbf{q}_0\rangle_1 \quad (2.8)$$

and the NN t-matrix as given in the subsystem (23)

$$t \equiv t_1 \equiv t_{23}. \quad (2.9)$$

The index 1 is the convenient and usual notation [7] to single out the pair (23). Similarly we shall denote $t_2 \equiv t_{31}$ and $t_3 \equiv t_{12}$. The permutation operator P is given as

$$P = P_{12}P_{23} + P_{13}P_{23}. \quad (2.10)$$

Next we define

$$\begin{aligned} |\Phi\rangle_2 &\equiv P_{12}P_{23}|\Phi\rangle_1 \\ |\Phi\rangle_3 &\equiv P_{13}P_{23}|\Phi\rangle_1 \end{aligned} \quad (2.11)$$

Applying P to the left and right one obtains for the first term on the right hand side of Eq. (2.6)

$$\begin{aligned} \langle \Phi | P(t - t^\dagger) P | \Phi \rangle &= {}_3\langle \Phi | t - t^\dagger | \Phi \rangle_2 + {}_2\langle \Phi | t - t^\dagger | \Phi \rangle_2 \\ &\quad + {}_3\langle \Phi | t - t^\dagger | \Phi \rangle_3 + {}_2\langle \Phi | t - t^\dagger | \Phi \rangle_3. \end{aligned} \quad (2.12)$$

An immediate consequence of Eq. (2.11) and the antisymmetry of the deuteron state $|\varphi_d\rangle$ is

$$|\Phi\rangle_3 = -P_{23}|\Phi\rangle_2. \quad (2.13)$$

Consequently one has

$$\begin{aligned} {}_3\langle \Phi | t - t^\dagger | \Phi \rangle_3 &= {}_2\langle \Phi | P_{23}(t - t^\dagger) P_{23} | \Phi \rangle_2 = {}_2\langle \Phi | t - t^\dagger | \Phi \rangle_2 \\ {}_3\langle \Phi | t - t^\dagger | \Phi \rangle_2 &= -{}_2\langle \Phi | P_{23}(t - t^\dagger) | \Phi \rangle_2 = {}_2\langle \Phi | t - t^\dagger | \Phi \rangle_3. \end{aligned} \quad (2.14)$$

Here we used the symmetry of t under exchange of particles 2 and 3.

As final result we obtain for the first term on the right hand side of Eq. (2.6), the first order term of the multiple scattering expansion for the nd total cross section

$$\begin{aligned} \langle \Phi | P(t - t^\dagger) P | \Phi \rangle &= 2 \{ {}_2\langle \Phi | t - t^\dagger | \Phi \rangle_2 + {}_2\langle \Phi | t - t^\dagger | \Phi \rangle_3 \} \\ &= 2 {}_2\langle \Phi | (t - t^\dagger) (1 - P_{23}) | \Phi \rangle_2 \end{aligned} \quad (2.15)$$

It is a straightforward but tedious algebra to evaluate Eq. (2.15) in the high energy limit. The derivation is sketched in Appendix A. Thus, the first order term in the multiple

scattering expansion gives in the high energy limit the following contribution to the total nd cross section

$$\sigma_{nd,\text{tot}}^{(1)} = \sigma_{np}^{\text{tot}} + \sigma_{nn}^{\text{tot}}. \quad (2.16)$$

The high energy limit is defined as the projectile momentum q_0 being much larger than the typical momenta inside the deuteron. Thus Eq. (2.16) shows that in the high energy limit the total cross section for nd scattering in first order in the NN t -matrix is indeed given as the sum of the total cross sections for np and nn scattering. This corresponds to the naive expectation, where the projectile nucleon scatters independently from both constituents of the deuteron.

Next we study the rescattering processes of second order in t as given in Eq. (2.7). Working out the permutations the first term of the right hand side of Eq. (2.7) can be written as

$$\begin{aligned} \langle \Phi | P(t - t^\dagger) P G_0 t P | \Phi \rangle &= 2 \{ {}_2 \langle \Phi | (t - t^\dagger) G_0 t_3 (|\Phi\rangle_1 + |\Phi\rangle_2) \\ &\quad + 2 \{ {}_2 \langle \Phi | (t - t^\dagger) G_0 t_2 (|\Phi\rangle_1 + |\Phi\rangle_3) \}. \end{aligned} \quad (2.17)$$

Similarly the remaining term in Eq. (2.7) yields

$$\begin{aligned} \langle \Phi | P t^\dagger P (G_0 - G_0^*) t P | \Phi \rangle &= -4\pi i \{ {}_2 \langle \Phi | t^\dagger \delta(E - H_0) t_3 (|\Phi\rangle_1 + |\Phi\rangle_2) \\ &\quad + {}_2 \langle \Phi | t^\dagger \delta(E - H_0) t_2 (|\Phi\rangle_1 + |\Phi\rangle_3) \}. \end{aligned} \quad (2.18)$$

The analytic evaluation of the high energy limit is even more tedious and is sketched in Appendix B. The leading contribution of the terms given in Eq. (2.7), second order in t in the multiple scattering expansion to the total nd cross section, is given by

$$\begin{aligned} \sigma_{nd,\text{tot}}^{(2)} &= -\frac{1}{4\pi} \sum_{l'l'} i^{l'-l} \int_0^\infty dr \varphi_l(r) \varphi_{l'}(r) \times \\ &\quad [2 C(11l, 1, -1) C(11l', 1, -1) \\ &\quad \{ -\frac{1}{2} \left(\frac{4m}{3q_0} \right)^2 (2\pi)^6 \left(\frac{1}{2} (\text{Im} \langle -\frac{3}{4} \mathbf{q}_0 \frac{1}{2} \frac{1}{2} np | t | \frac{3}{4} \mathbf{q}_0 \frac{1}{2} \frac{1}{2} np \rangle_a)^2 \right. \\ &\quad - \frac{1}{2} (\text{Re} \langle -\frac{3}{4} \mathbf{q}_0 \frac{1}{2} \frac{1}{2} np | t | \frac{3}{4} \mathbf{q}_0 \frac{1}{2} \frac{1}{2} np \rangle_a)^2 \\ &\quad + \frac{1}{2} (\text{Im} \langle -\frac{3}{4} \mathbf{q}_0 - \frac{1}{2} \frac{1}{2} np | t | \frac{3}{4} \mathbf{q}_0 \frac{1}{2} - \frac{1}{2} np \rangle_a)^2 \\ &\quad - \frac{1}{2} (\text{Re} \langle -\frac{3}{4} \mathbf{q}_0 - \frac{1}{2} \frac{1}{2} np | t | \frac{3}{4} \mathbf{q}_0 \frac{1}{2} - \frac{1}{2} np \rangle_a)^2 \\ &\quad + \text{Re} \langle \frac{3}{4} \mathbf{q}_0 \frac{1}{2} \frac{1}{2} np | t | \frac{3}{4} \mathbf{q}_0 \frac{1}{2} \frac{1}{2} np \rangle_a \text{Re} \langle \frac{3}{4} \mathbf{q}_0 \frac{1}{2} \frac{1}{2} nn | t | \frac{3}{4} \mathbf{q}_0 \frac{1}{2} \frac{1}{2} nn \rangle_a \\ &\quad \left. + \text{Re} \langle \frac{3}{4} \mathbf{q}_0 \frac{1}{2} - \frac{1}{2} nn | t | \frac{3}{4} \mathbf{q}_0 \frac{1}{2} - \frac{1}{2} nn \rangle_a \text{Re} \langle \frac{3}{4} \mathbf{q}_0 \frac{1}{2} - \frac{1}{2} np | t | \frac{3}{4} \mathbf{q}_0 \frac{1}{2} - \frac{1}{2} np \rangle_a \right\} \\ &\quad + C(11l, 00) C(11l', 00) \\ &\quad \{ -\frac{1}{2} \left(\frac{4m}{3q_0} \right)^2 (2\pi)^6 \left(\frac{1}{2} (\text{Im} \langle -\frac{3}{4} \mathbf{q}_0 \frac{1}{2} - \frac{1}{2} np | t | \frac{3}{4} \mathbf{q}_0 \frac{1}{2} - \frac{1}{2} np \rangle_a)^2 \right. \\ &\quad \left. - \frac{1}{2} (\text{Re} \langle -\frac{3}{4} \mathbf{q}_0 \frac{1}{2} - \frac{1}{2} np | t | \frac{3}{4} \mathbf{q}_0 \frac{1}{2} - \frac{1}{2} np \rangle_a)^2 \right) \end{aligned}$$

$$\begin{aligned}
& +\text{Im}\langle -\frac{3}{4}\mathbf{q}_0 \frac{11}{22}np|t|\frac{3}{4}\mathbf{q}_0 \frac{11}{22}np\rangle_a \text{Im}\langle -\frac{3}{4}\mathbf{q}_0 - \frac{11}{22}np|t|\frac{3}{4}\mathbf{q}_0 \frac{1}{2} - \frac{1}{2}np\rangle_a \\
& -\text{Im}\langle \frac{3}{4}\mathbf{q}_0 \frac{1}{2} - \frac{1}{2}np|t|\frac{3}{4}\mathbf{q}_0 - \frac{11}{22}np\rangle_a \text{Im}\langle \frac{3}{4}\mathbf{q}_0 \frac{1}{2} - \frac{1}{2}nn|t|\frac{3}{4}\mathbf{q}_0 - \frac{11}{22}nn\rangle_a \\
& +\text{Re}\langle \frac{3}{4}\mathbf{q}_0 \frac{11}{22}np|t|\frac{3}{4}\mathbf{q}_0 \frac{11}{22}np\rangle_a \text{Re}\langle \frac{3}{4}\mathbf{q}_0 \frac{1}{2} - \frac{1}{2}nn|t|\frac{3}{4}\mathbf{q}_0 \frac{1}{2} - \frac{1}{2}nn\rangle_a \\
& +\text{Re}\langle \frac{3}{4}\mathbf{q}_0 \frac{11}{22}nn|t|\frac{3}{4}\mathbf{q}_0 \frac{11}{22}nn\rangle_a \text{Re}\langle \frac{3}{4}\mathbf{q}_0 \frac{1}{2} - \frac{1}{2}np|t|\frac{3}{4}\mathbf{q}_0 \frac{1}{2} - \frac{1}{2}np\rangle_a \\
& -\text{Re}\langle -\frac{3}{4}\mathbf{q}_0 \frac{11}{22}np|t|\frac{3}{4}\mathbf{q}_0 \frac{11}{22}np\rangle_a \text{Re}\langle -\frac{3}{4}\mathbf{q}_0 - \frac{11}{22}np|t|\frac{3}{4}\mathbf{q}_0 \frac{1}{2} - \frac{1}{2}np\rangle_a \\
& +\text{Re}\langle \frac{3}{4}\mathbf{q}_0 \frac{1}{2} - \frac{1}{2}np|t|\frac{3}{4}\mathbf{q}_0 - \frac{11}{22}np\rangle_a \text{Re}\langle \frac{3}{4}\mathbf{q}_0 \frac{1}{2} - \frac{1}{2}nn|t|\frac{3}{4}\mathbf{q}_0 - \frac{11}{22}nn\rangle_a) \} \\
& - \frac{1}{4\pi} \sum_{ll'} i^{l'-l} \int_0^\infty dr \varphi_l(r) \varphi_{l'}(r) \times \\
& \quad [2 C(11l, 1, -1) C(11l', 1, -1) \\
& \quad \{ \frac{1}{2} (\sigma_{np}^{\text{tot}}(\frac{11}{22}) \sigma_{nn}^{\text{tot}}(\frac{11}{22}) + \sigma_{np}^{\text{tot}}(\frac{1}{2} - \frac{1}{2}) \sigma_{nn}^{\text{tot}}(\frac{1}{2} - \frac{1}{2})) \\
& \quad + C(11l, 00) C(11l', 00) \\
& \quad \{ \frac{1}{2} (\sigma_{np}^{\text{tot}}(\frac{11}{22}) \sigma_{nn}^{\text{tot}}(\frac{1}{2} - \frac{1}{2}) + \sigma_{np}^{\text{tot}}(\frac{1}{2} - \frac{1}{2}) \sigma_{nn}^{\text{tot}}(\frac{11}{22})) \} \\
& \equiv \sigma_I^{(2)} + \sigma_{II}^{(2)} \tag{2.19}
\end{aligned}$$

Here the sum over l, l' denote the S and D-wave contributions of the deuteron wave functions $\varphi_l(r)$. Further occur the imaginary and real parts of the forward and backward two-nucleon scattering amplitudes (nn or np) with specified spin magnetic quantum numbers in the initial and final states. The index a denotes antisymmetrization without the factor $\frac{1}{\sqrt{2}}$. The terms of second order in t give rise to Eq. (2.19), a quite complicated expression exhibiting the interferences due to spin and isospin degrees of freedom. The part $\sigma_I^{(2)}$ related to the first square bracket in Eq. (2.19) contains real and imaginary parts of the NN scattering amplitudes and has positive as well as negative contributions. Only a numerical evaluation of these terms as function of the scattering energy can give insight about the size and energy dependence of these terms. The part $\sigma_{II}^{(2)}$ related to the second square bracket contains due the optical theorem a product of two NN total cross sections. That part $\sigma_{II}^{(2)}$ is negative and reduces the term of first order in the multiple scattering expansions, the sum of the two NN total cross sections. This is naturally called shadowing effect.

Neglecting spin and isospin dependencies and consequently the D-wave admixture in the deuteron, and further neglecting the backward amplitudes that expression given in Eq. (2.19) reduces to the much simpler ones which are given in [6] for 3 bosons.

III. DISCUSSION OF THE RESULTS OF THE FADDEEV CALCULATIONS AND OF THE HIGH ENERGY LIMIT

For calculating the nd total cross section we employ the most recent NN potentials, namely CD-Bonn [9], AV18 [10], Nijm I and II [11]. Those potentials are optimally fitted to

the Nijmegen data basis up to 350 MeV nucleon laboratory energy. The Faddeev equation Eq. (2.1) is solved in momentum space in a partial wave decomposed form. For a description of the technical details of the calculations we refer to Ref. [8]. In Fig. 1 we compare the calculated nd total cross section based on the CD-Bonn potential with the data. The experimental data are obtained by adding the separately measured values of the hydrogen cross section and the deuterium-hydrogen cross section difference [1]. The figure shows that the theoretical calculation describes the data very well at the lower energies but falls below the data at higher energies. The calculation begins to underestimate the data around 100 MeV by about 4%, and this discrepancy increases to about 11% at 300 MeV.

The calculation presented in Fig. 1 employs in the two-nucleon subsystem angular momenta up to $j_{max}=4$. This is sufficient if we are satisfied with a calculational accuracy of 1%, which corresponds to the size of the experimental error. In order to demonstrate the dependence of the numerical accuracy of our calculations, we show in Table I for a few energies in the relevant energy regime the convergence of the total cross section as function of j_{max} , the maximum angular momentum of the two-nucleon subsystem. In the 3N calculations two-nucleon angular momenta larger than j_{max} are put to zero. We see that $j_{max} = 4$ is sufficient, if we are satisfied with an accuracy of 1%. Next we demonstrate the stability of our theoretical result under the exchange of the NN potentials. This is shown in Table II. Clearly within an accuracy of 1% the predictions of those four essentially phase equivalent potentials agree with each other. From this we can conclude that the deviation of the calculation from the data at higher energies, which is shown in Fig. 1 is independent from the NN interaction employed.

In order to gain some insight how the total nd cross section is build up, the individual contributions of first, second and third order in the multiple scattering expansion of the elastic amplitude are compared. In Fig. 2 we present the total cross section calculated in first order, successively add the contributions of the second and third order and compare those results with the full calculation. The figure shows that the first order in the multiple scattering expansion is larger than the full result at all energies. The second order contribution enhances the cross section below about 130 MeV and decreases it at the higher energies. We also see that at energies below about 200 MeV the third order term is significantly larger than the second order term, and thus that rescattering of higher order is very important. Only above 200 MeV the third order contribution becomes negligible. Here the small correction of the second order rescattering process becomes sufficient to describe together with the first order contribution the full solution of the Faddeev equation. Around 300 MeV the first two terms in the multiple scattering expansion of the scattering amplitude are sufficient to describe the total cross section.

As a next step we consider the high energy limit of the first and second order terms of the multiple scattering expansion as derived in Sec. II. The first order term results in a sum of the total cross section for np and nn scattering. The high energy limit of the second order term is given in Eq. (2.19). In this equation we already indicate that this term consists of two parts, one which consists of products of real and imaginary parts of the NN t-matrix, and one which is due to the optical theorem proportional to products of NN total cross sections. The latter term is negative and can be considered as shadowing effect. The contributions of the different terms of the high energy limit are shown in Fig. 3. We show the individual contributions up to a laboratory energy of 800 MeV in order to get a better

insight into their energy dependence. The contribution of the sum of $\sigma_{np} + \sigma_{nn}$ is by far dominant. The calculation shows that $\sigma_I^{(2)}$ is always positive and thus enhances the total cross section. Thus this term could be viewed as anti-shadowing effect. The term $\sigma_{II}^{(2)}$ is always negative. We see that $\sigma_I^{(2)}$ falls off faster as function of the energy than $\sigma_{II}^{(2)}$. This interplay of the different contributions to the high energy limit of the second order term in the multiple scattering expansion leads to an enhancement of the total nd cross section below about 400 MeV and a weakening above compared to the sum of the np and nn total cross sections. Thus only above 400 MeV the second order term in the elastic amplitude leads in the high energy limit to a shadowing effect as it is familiar from older estimates within the framework of Glauber theory. This is shown in Fig. 4. The dashed line gives the contribution of the sum of $\sigma_{np} + \sigma_{nn}$. To this sum the term $\sigma_I^{(2)}$ is added and given by the dotted line and enhances the total cross section. Then we add in addition $\sigma_{II}^{(2)}$ leading to the solid line.

It is now interesting to compare those results obtained from the first two terms of the multiple scattering expansion in the high energy limit with the corresponding contributions calculated exactly with the Faddeev framework. This comparison is summarized in Table III. The second column gives the exact Faddeev result as reference. It should be noted that all results given in Table III are calculated using $j_{max}=4$ in the two-nucleon subsystem. Starting at 100 MeV we compare the exact first order result to its high energy limit, the sum of the np and nn total cross sections, as given in Eq. (2.16). The table shows that this sum is larger than the exact first order term for 140 MeV and higher. In fact, the difference increases with increasing energy. In the case of three bosons interacting via Malfliet-Tjon type forces (acting in **all** partial waves) this difference vanishes around 300 MeV and the asymptotic expression acquires its validity here [6]. Apparently, the three nucleon system with realistic forces behaves differently. It would be very interesting to find out at which energy the first order term will reach the asymptotic form. This interest is however restricted to the context of a mathematical model of potential scattering, since the standard NN forces loose their physical meaning above pion-production threshold.

Next we compare the exact second order result to the expression of the high energy limit as given in Eq. (2.19). First, the exact second order result of the Faddeev formalism is a small correction to the first order result. At lower energies it is additive and changes sign around 150 MeV, which then leads to a reduction of the cross section. As can be seen in Fig. 3, the second order term in the high energy limit exhibits this behavior only around 400 MeV. Comparing the sum of first and second order terms of the exact Faddeev calculation to the corresponding term in the high energy limit (column 9 which is the sum of the terms in columns 6-8 in Table III) shows that the high energy limit is always larger in the energy region under consideration. At 300 MeV the difference for the combined results in those orders is still 8%, and thus the high energy limit is not yet quantitatively valid.

As remark we would like to add that the asymptotic form requires higher NN force components than $j_{max}=4$. For the study presented in Table III we kept the angular momenta in the two-nucleon system fixed at this value in order to compare with the Faddeev results. The two-nucleon t matrices underlying the calculations presented in Fig. 3, however, employ up to $j_{max}=15$ in order to obtain a converged result at 800 MeV. In the case of the high energy limit this can be easily achieved, since only the NN on-shell amplitudes enter.

IV. ESTIMATE OF THREE-NUCLEON FORCE AND RELATIVISTIC CORRECTIONS

In this section we want to study the effect of three nucleon forces (3NF) on the total nd cross section and give a very simple estimate on the size of relativistic effects. The inclusion of 3NF in 3N continuum Faddeev calculations has been formulated in Ref. [12], superseding a previous formulation given in Ref. [8]. The newer formulation is formally more elegant and numerically more efficient and is used in our calculations. The inclusion of 3NF generalizes Eq. (2.1) to

$$T|\Phi\rangle = tP|\Phi\rangle + (1 + tG_0)V_4^{(1)}(1 + P)|\Phi\rangle + tPG_0T|\Phi\rangle + (1 + tG_0)V_4^{(1)}(1 + P)G_0T|\Phi\rangle, \quad (4.1)$$

where $V_4^{(1)}$ is that part of the 3NF, which is symmetric under exchange of particles 2 and 3. The total 3NF then has the form

$$V_4 = V_4^{(1)} + V_4^{(2)} + V_4^{(3)}, \quad (4.2)$$

and is totally symmetric. The full breakup operator as given in Eq. (2.2) keeps its form, whereas the operator for elastic nd scattering changes to

$$U = PG_0^{-1} + V_4^{(1)}(1 + P) + PT + V_4^{(1)}(1 + P)G_0T. \quad (4.3)$$

The optical theorem given in Eq. (2.4) stays of course valid.

The numerical evaluation of Eq. (4.1) is quite demanding, since in contrast to the 3N bound state one needs the partial wave projected momentum space representation of $V_4^{(1)}$ now for both parities and, in addition, for total 3N angular momenta larger than $J = 1/2$. At a projectile energy $E_{lab}^n = 200$ MeV we checked that total angular momenta up to $J = 9/2$ were needed. The calculation of the three-nucleon force matrix elements for such high angular momenta became possible due to the new partial wave decomposition for the three-nucleon force introduced in [13]. Of course, NN forces contribute significantly up to $J = 25/2$ to 3N scattering states. In our calculations we employ the Tucson-Melbourne force [14], which has been adjusted individually to the ${}^3\text{H}$ binding energy for each of the different modern NN forces [15]. The results presented in this paper are based on the CD-Bonn potential and the corresponding parameters of the Tucson-Melbourne force.

In a previous study we found that 3N force effects are responsible for filling the minima in the angular distribution of elastic nd scattering, especially at higher energies [16]. Though the effect is seen only in the minima of the differential cross sections, and thus is small in magnitude, one might expect traces thereof in the integrated quantity, the total cross section. Corresponding effect to those in the elastic angular distribution might also occur in 3N breakup processes, over which is also integrated when calculating the total cross section. This is indeed the case as shown in Fig. 5. The effect of the 3N force enhances the total nd cross section calculated with NN forces only by about 4%. It is interesting to note that this enhancement is almost independent of the energy when considering the energy regime between 100 and 300 MeV. It is also obvious from the figure that the 3N force effects included here are not strong enough to bridge the gap between the calculation based on 2N forces only

and the data. However, one should keep in mind that the Tucson-Melbourne 3NF model is just one model, and theory as well as application of 3N forces is just at the beginning.

A second effect, which can be expected to appear especially at higher energies is an effect due to relativity. A generally accepted framework for carrying out relativistic 3N scattering calculations does not yet exist. Thus we restrict ourselves to a very simple estimate of a relativistic kinematic effect. Due to the optical theorem the total cross section is given as

$$\sigma_{tot}^{nd} \propto \frac{1}{|j|} \text{Im} \langle \Phi | U | \Phi \rangle, \quad (4.4)$$

where $|j|$ is the incoming current density. If we neglect possible changes of $\text{Im} \langle \Phi | U | \Phi \rangle$ in going from a nonrelativistic to a relativistic formulation, the ratio of the relativistic to the nonrelativistic total cross section is simply given by

$$\frac{\sigma_{tot,rel}^{nd}}{\sigma_{tot,nr}^{nd}} = \frac{|j|_{nr}}{|j|_{rel}} = \frac{E_n E_d}{p_n^{rel}(E_n + E_d)} / \frac{m_n m_d}{p_n^{nr}(m_n + m_d)}. \quad (4.5)$$

Here, E_n and E_d are the relativistic kinetic energies of the neutron and the deuteron in the c.m. system, and p_n^{rel} is the relativistic c.m. momentum. The other terms are obviously the nonrelativistic approximations thereof. This ratio given in Eq. (4.5) is easily evaluated and leads to an increase of the total nd cross section, namely an increase of about 3% at 100 MeV and about 7% at 250 MeV. Calculations based on 2N forces only, which include this relativistic effect, are shown at various energies in Fig. 5. Again, these additional effects enhance the total cross section and bring the calculation closer to the data. It is also clear that this effect does not constitute a relativistic theory, since the forward scattering amplitude is still calculated entirely nonrelativistically. However, both effects, the one caused by inclusion of a 3NF model and the simple estimate of a relativistic effect, are roughly similar in magnitude, and when added up would come close to the data in the higher energy regime. It should be also noted that at lower energies, the added effects would overpredict the data.

V. SUMMARY

In view of new precise experimental information on the total nd cross section fully converged Faddeev calculations based on the most modern NN forces are carried out at projectile energies between 10 and 300 MeV. For the Faddeev calculations a strictly nonrelativistic treatment is employed. The calculations show that the results for the total nd cross section do not depend on the choice among the most recent phase-equivalent potentials.

In order to obtain more insight into the behavior of the multiple scattering series for the nd total cross section, we study its convergence within the Faddeev framework. Below about 200 MeV projectile energy rescattering of higher order is very important, as can be concluded from the fact that here the third order contribution of the multiple scattering series is significantly larger in magnitude than the second order. Only around 300 MeV the first two terms in the multiple scattering expansion are sufficient to describe the total nd cross section.

In order to obtain analytical insight we investigate the first terms of the multiple scattering series for the forward elastic nd scattering amplitude resulting from the Faddeev

equations in the high energy limit. Although the treatment is purely nonrelativistic and enters far into the region where relativity is expected to be important, we think it is interesting to know the asymptotic behavior at high energies for pure potential models without absorption. Absorption processes (particle production) occurring in a relativistic context will change the results presented here. In accordance with the naive expectation, we extract from the first order term in the multiple scattering series the sum of the total cross sections for np and nn scattering, and from the second order term a shadowing effect proportional to products of the total NN cross sections. The shadowing contribution is negative and reduces the total nd cross section. However, we also find positive terms proportional to products of real and imaginary parts of spin dependent NN forward and backward scattering amplitudes. Those terms provide an overall enhancement of the nd total cross section, but vanish faster with energy than the shadowing term. At projectile energies above 400 MeV the shadowing is the dominant second order effect.

A comparison of the theoretical calculations based on a nonrelativistic Faddeev framework with two-nucleon forces only and the experimental observables exhibits a discrepancy with respect to the nd data, which starts around 100 MeV with a few percent and reaches about 10% at 300 MeV. Possible corrections can be due to either three-nucleon forces or relativistic effects or both. We calculated the effect of the Tucson-Melbourne 3N force on the total nd cross section and find that in the energy regime between 100 and 300 MeV this 3NF model provides an overall enhancement of the total cross section of $\sim 4\%$. This is consistent with previous studies, which found that the minima of the elastic scattering angular distribution are filled in when this 3NF is taken into consideration. In the total cross section this effect is not large enough to bring the present calculations close to the data, but the trend is in the right direction.

A second effect, which can be expected to appear especially at higher energies is due to relativity. We carry out a simple estimate of effects due to relativistic kinematics, and find that these corrections enhance the total nd cross section about 7% at 250 MeV, while being much smaller at lower energies. Again, those corrections go into the right direction with respect to the data. However, we do not suggest that our estimate is the complete solution of the problem, since in our calculation the forward scattering amplitude is still calculated entirely nonrelativistically.

Both our estimates of corrections to our nonrelativistic Faddeev calculations based on 2N forces suggest, that effects due to 3N forces as well as relativistic effects become non negligible at higher energies. This calls for a strong effort to progress theoretical developments of a theory of 3N forces as well as a relativistic framework for 3N scattering.

ACKNOWLEDGMENTS

This work was performed in part under the auspices of the U. S. Department of Energy under contracts No. DE-FG02-93ER40756 with Ohio University, the NATO Collaborative Research Grant 960892, the National Science Foundation under Grant No. INT-9726624 and the Deutsche Forschungsgemeinschaft. The work of D.H. was supported in part by the U.S. Department of Energy and in part by the Deutsche Forschungsgemeinschaft under contract Hu 746/1-3. We thank the Ohio Supercomputer Center (OSC) for the use of their facilities under Grant No. PHS229 and the Höchstleistungsrechenzentrum (HLRZ) Jülich for the use of their T90 and T3E computers.

REFERENCES

- [1] W.P. Abfalterer et al., Phys. Rev. Lett. **81**, 57 (1998).
- [2] R.J. Glauber, Phys. Rev. **100**, 242 (1955); R.J. Glauber in Lectures in Theoretical Physics, Vol.1, edited by W. Brittin and L.G. Dunham, Interscience Publ., New York, 1959).
- [3] C.J. Joachain, ‘Quantum Collision Theory’ (North-Holland Physics 1987)
- [4] H. Frauenfelder, E.M. Henley, ‘Subatomic Physics’, Prentice Hall, 1991, p. 168.
- [5] E.S.Abers, H.Burkhardt, V.L.Teplitz, C.Wilkin, Nuovo Cim. **XLII A**, 365 (1969).
- [6] Ch. Elster, W. Schadow, H. Kamada, W. Glöckle, Phys. Rev. **C58**, 3109 (1998).
- [7] W. Glöckle, The quantum mechanical few body problem, Springer Verlag 1983.
- [8] W. Glöckle, H. Witała, D. Hüber, H. Kamada, and J. Golak, Phys. Rep. **274**, 107 (1996).
- [9] R. Machleidt, F. Sammarruca, and Y. Song, Phys. Rev. **C53**, R1483 (1996).
- [10] R. B. Wiringa, V. G. J. Stoks, and R. Schiavilla, Phys. Rev. **C51**, 38 (1995).
- [11] V. G. J. Stoks, R. A. M. Klomp, C. P. F. Terheggen, and J. J. de Swart, Phys. Rev. **C49**, 2950 (1994).
- [12] D. Hüber, H. Kamada, H. Witała, and W. Glöckle, Acta Phys. Pol. **B28**, 1677 (1997).
- [13] D.Hüber, H.Witała, A.Nogga, W.Glöckle, and H.Kamada, Few-Body Systems **22**, 107 (1997)
- [14] S.A. Coon and W. Glöckle, Phys. Rev. **C23**, 1790 (1981); S.A. Coon *et al.*, Nucl. Phys. **A317** 242 (1979).
- [15] A. Nogga, D. Hüber, H. Kamada, and W. Glöckle, Phys. Lett. **B409**, 19 (1997).
- [16] H. Witała, W. Glöckle, D. Hüber, J. Golak, and H. Kamada, Phys. Rev. Lett. **81**, 1183 (1998).

APPENDIX A: THE HIGH ENERGY LIMIT OF THE FIRST ORDER TERM IN THE NN T-MATRIX

To evaluate the first order term of the multiple scattering expansion for the total cross section in the high energy limit we consider

$$X_1 \equiv {}_2\langle \Phi | (t - t^\dagger) (1 - P_{23}) | \Phi \rangle_2. \quad (\text{A1})$$

The completeness relation in the three-nucleon space is given by

$$1 = \sum_{m_1 m_2 m_3} \sum_{\nu_1 \nu_2 \nu_3} \int d^3 p d^3 q$$

$$| \mathbf{p} m_2 m_3 \nu_2 \nu_3 \rangle | \mathbf{q} m_1 \nu_1 \rangle \langle \mathbf{p} m_2 m_3 \nu_2 \nu_3 | \langle \mathbf{q} m_1 \nu_1 | \quad (\text{A2})$$

Here \mathbf{p} and \mathbf{q} are standard Jacobi momenta, m_i the spin magnetic quantum numbers and ν_i the corresponding isospin quantum numbers of the three nucleons. In that notation the channel state $|\Phi\rangle_2$ reads

$$|\Phi\rangle_2 = |\varphi_d m_d \nu_d \rangle | \mathbf{q}_0 m_N \nu_N \rangle. \quad (\text{A3})$$

We also need a change of basis

$${}_2 \langle \mathbf{p} m_3 m_1 \nu_3 \nu_1 \mathbf{q} m_2 \nu_2 | \mathbf{p}' m'_2 m'_3 \nu'_2 \nu'_3 \mathbf{q}' m'_1 \nu'_1 \rangle_1$$

$$= \delta(\mathbf{p}' - \frac{1}{2} \mathbf{q}' - \mathbf{q}) \delta(\mathbf{p} + \mathbf{q}' + \frac{1}{2} \mathbf{q}) \prod_{i=1}^3 \delta_{m_i m'_i} \prod_{i=1}^3 \delta_{\nu_i \nu'_i} \quad (\text{A4})$$

and the explicit expression for the deuteron state

$$\langle \mathbf{p} m_3 m_1 \nu_3 \nu_1 | \varphi_d \rangle =$$

$$\frac{(-)^{\frac{1}{2} - \nu_3}}{\sqrt{2}} \delta_{\nu_1, -\nu_3} \sum_{lm_l} (l11, m_l m_d - m_l)$$

$$Y_{lm_l}(\hat{p}) \left(\frac{1}{2} \frac{1}{2} 1, m_3 m_1 m_d - m_l \right) \varphi_l(p) \quad (\text{A5})$$

As an immediate step one finds after a suitable substitution of integration variables

$${}_2 \langle \Phi | t - t^\dagger | \Phi \rangle_2 = \sum_{m_1 m_3} \sum_{m'_3} \sum_{\nu_1 \nu_3} \sum_{\nu'_3} \int d^3 z \langle \varphi_d | -\mathbf{z} m_3 m_1 \nu_3 \nu_1 \rangle$$

$$\langle \frac{3}{4} \mathbf{q}_0 + \frac{1}{2} \mathbf{z} m_N m_3 \nu_N \nu_3 | t - t^\dagger | \frac{3}{4} \mathbf{q}_0 + \frac{1}{2} \mathbf{z} m_N m'_3 \nu_N \nu'_3 \rangle$$

$$\langle -\mathbf{z} m'_3 m_1 \nu'_3 \nu_1 | \varphi_d \rangle$$

If the projectile momentum $\frac{3}{4} \mathbf{q}_0$ is much larger than typical momenta \mathbf{z} occurring in the deuteron state, one can take the NN t-matrices out of the integral and obtains

$$\begin{aligned}
{}_2 \langle \Phi | t - t^\dagger | \Phi \rangle_2 &\xrightarrow{\frac{3}{4}q_0 \rightarrow \infty} \\
&\sum_{m_1 m_3} \sum_{m'_3} \sum_{\nu_1 \nu_3} \sum_{\nu'_3} \langle \frac{3}{4} \mathbf{q}_0 m_N m_3 \nu_N \nu_3 | t - t^\dagger | \frac{3}{4} \mathbf{q}_0 m_N m'_3 \nu_N \nu'_3 \rangle \times \\
&\int d^3 z \langle \varphi_d | -\mathbf{z} m_3 m_1 \nu_3 \nu_1 \rangle \langle -\mathbf{z} m'_3 m_1 \nu'_3 \nu_1 | \varphi_d \rangle. \quad (\text{A6})
\end{aligned}$$

Here the energy argument of the t matrices is given by

$$\begin{aligned}
\varepsilon &\equiv E - \frac{3}{4m} \left(-\frac{1}{2} \mathbf{q}_0 + \mathbf{z}\right)^2 \\
&= \varepsilon_d + \frac{3}{4m} \mathbf{q}_0^2 - \frac{3}{4m} \left(\frac{1}{4} \mathbf{q}_0^2 - \mathbf{q}_0 \cdot \mathbf{z} + \mathbf{z}^2\right) \\
&= \varepsilon_d + \frac{1}{m} \left(\frac{3}{4} \mathbf{q}_0\right)^2 + \frac{3}{4m} \mathbf{q}_0 \cdot \mathbf{z} - \frac{3}{4m} \mathbf{z}^2 \\
&\xrightarrow{\frac{3}{4}q_0 \rightarrow \infty} \frac{1}{m} \left(\frac{3}{4m} \mathbf{q}_0\right)^2. \quad (\text{A7})
\end{aligned}$$

Thus in the high energy limit we only encounter on-shell NN t-matrices.

Using Eq.(A5) we find

$$\begin{aligned}
{}_2 \langle \Phi | t - t^\dagger | \Phi \rangle_2 &\longrightarrow \sum_{m_1 m_3} \sum_{\nu_1} \langle \frac{3}{4} \mathbf{q}_0 m_N m_3 \nu_N, -\nu_1 | t - t^\dagger | \frac{3}{4} \mathbf{q}_0 m_N m_3 \nu_N, -\nu_1 \rangle \\
&\frac{1}{2} \sum_l \int_0^\infty dp p^2 \varphi_l^2(p) C(l11, m_d - m_3 - m_1, m_3 + m_1)^2 \\
&C\left(\frac{1}{2} \frac{1}{2} 1, m_3 m_1\right)^2. \quad (\text{A8})
\end{aligned}$$

The next step is to introduce properly antisymmetrized NN states in the NN t-matrix. This comes automatically of course, since the form X_1 contains the operation $(1 - P_{23})$. Taking this into account we find altogether for the expression Eq. (2.15)

$$\begin{aligned}
\langle \Phi | P(t - t^\dagger) P | \Phi \rangle &\longrightarrow \sum_{m_1 m_3} \sum_{\nu_1} n_a \langle \frac{3}{4} \mathbf{q}_0 m_N m_3 \nu_N, -\nu_1 | t - t^\dagger | \frac{3}{4} \mathbf{q}_0 m_N m_3 \nu_N, -\nu_1 \rangle_{n_a} \\
&\times \sum_l \int_0^\infty dp p^2 \varphi_l^2(p) C(l11, m_d - m_3 - m_1, m_3 + m_1)^2 \\
&C\left(\frac{1}{2} \frac{1}{2} 1, m_3 m_1\right)^2. \quad (\text{A9})
\end{aligned}$$

Here the antisymmetrized and normalized free NN state is given by

$$|\mathbf{p} m_2 m_3 \nu_2 \nu_3 \rangle_{n_a} \equiv \frac{1}{\sqrt{2}} (1 - P_{23}) |\mathbf{p} m_2 m_3 \nu_2 \nu_3 \rangle. \quad (\text{A10})$$

Finally we use the relation

$$t - t^\dagger = -2\pi i \frac{3}{4} q_0 \frac{m}{2} \sum_{m'_2 m'_3} \sum_{\nu'_2 \nu'_3} \int d\hat{p} V \left| \frac{3}{4} q_0 \hat{p} m'_2 m'_3 \nu'_2 \nu'_3 \right\rangle^{(+)} \langle \frac{3}{4} q_0 \hat{p} m'_2 m'_3 \nu'_2 \nu'_3 | V, \quad (\text{A11})$$

where the NN potential V is applied to the two-nucleon scattering states $|\dots\rangle^{(+)}$. Furthermore, the definition of the total NN cross section initiated by fixed magnetic spin and isospin quantum numbers is given by

$$\sigma_{\nu_N, -\nu_1}^{\text{tot}}(m_N, m_3) = (2\pi)^4 \left(\frac{m}{2}\right)^2 \sum_{m'_2 m'_3} \sum_{\nu'_2 \nu'_3} \int d\hat{p} |_{na} \langle \frac{3}{4} \mathbf{q}_0 m_N m_3 \nu_N, -\nu_1 | t | \frac{3}{4} q_0 \hat{p} m'_2 m'_3 \nu'_2 \nu'_3 \rangle|^2. \quad (\text{A12})$$

This inserted into Eq. (A9) and applying the relation given in Eq. (2.4) to the total nd cross section we arrive at

$$\begin{aligned} \sigma_{Nd}^{\text{tot}}(m_N, m_d \nu_N) &= \sum_{m_1 m_3} \sum_{\nu_1} \sigma_{\nu_N, -\nu_1}^{\text{tot}}(m_N, m_3) \\ &\times \sum_l \int_0^\infty dp p^2 \varphi_l^2(p) C(l11, m_d - m_3 - m_1, m_3 + m_1)^2 C\left(\frac{1}{2} \frac{1}{2}, m_3, m_1\right)^2. \end{aligned} \quad (\text{A13})$$

This is the contribution of the term Eq. (2.15) to the total nd cross section for initially polarized particles and a nucleon species of type ν_N . Averaging over the initial state polarizations one can perform the summations over m_d and m_N analytically and using the normalization conditions for the s- and d-wave parts of the deuteron wave function one ends up for a neutron induced process with

$$\sigma_{nd}^{\text{tot}} = \sigma_{np}^{\text{tot}} + \sigma_{nn}^{\text{tot}}. \quad (\text{A14})$$

APPENDIX B: THE HIGH ENERGY LIMITS OF THE SECOND ORDER TERMS IN THE NN T-MATRIX

To evaluate the second order term of the multiple scattering expansion for the total nd cross section in the high energy limit we consider

$$X_2 \equiv_2 \langle \Phi | (t - t^\dagger) G_0 t_3 | \Phi \rangle_1 \quad (\text{B1})$$

Corresponding steps to the ones carried out in Appendix A lead to

$$\begin{aligned} X_2 &= \sum_{m_1 m_3 \nu_1 \nu_3} \sum_{m'_2 m'_3 \nu'_2 \nu'_3} \sum_{m''_2 \nu''_2} \int d^3 z \int d^3 z' \langle \varphi_d | -\mathbf{z} m_3 m_1 \nu_3 \nu_1 \rangle \\ &\times \frac{\langle \frac{3}{4} \mathbf{q}_0 + \frac{1}{2} \mathbf{z} m_2^0 m_3 \nu_2^0 \nu_3 | t - t^\dagger | \frac{3}{4} \mathbf{q}_0 - \frac{1}{2} \mathbf{z} - \mathbf{z}' m'_2 m'_3 \nu'_2 \nu'_3 \rangle}{-|\epsilon_d| - \frac{1}{m}(z^2 + z'^2 + \mathbf{z} \cdot \mathbf{z}') + \frac{3}{2m}(\mathbf{z} + \mathbf{z}') \cdot \mathbf{q}_0 + i\epsilon} \\ &\times \langle -\frac{3}{4} \mathbf{q}_0 + \mathbf{z} + \frac{1}{2} \mathbf{z}' m_1 m'_2 \nu_1 \nu'_2 | t | \frac{3}{4} \mathbf{q}_0 + \frac{1}{2} \mathbf{z}' m''_1 m''_2 \nu''_1 \nu''_2 \rangle \\ &\langle -\mathbf{z}' m''_2 m'_3 \nu''_2 \nu'_3 | \varphi_d \rangle. \end{aligned} \quad (\text{B2})$$

Again we assume that $\frac{3}{4} q_0$ is much larger than the momenta z and z' in the deuteron state and find

$$\begin{aligned}
X_2 \longrightarrow & \sum_{m_1 m_3 \nu_1 \nu_3} \sum_{m'_2 m'_3 \nu'_2 \nu'_3} \sum_{m''_2 m''_3} \langle \frac{3}{4} \mathbf{q}_0 m_2^0 m_3 \nu_2^0 \nu_3 | t - t^\dagger | \frac{3}{4} \mathbf{q}_0 m'_2 m'_3 \nu'_2 \nu'_3 \rangle \\
& \times \langle -\frac{3}{4} \mathbf{q}_0 m_1 m'_2 \nu_1 \nu'_2 | t | \frac{3}{4} \mathbf{q}_0 m_1^0 m_2'' \nu_1^0 \nu_2'' \rangle \cdot \hat{I}, \tag{B3}
\end{aligned}$$

with

$$\hat{I} \equiv \int d^3 p \int d^3 p' \frac{\langle \varphi_d | -\mathbf{p} m_3 m_1 \nu_3 \nu_1 \rangle \langle -\mathbf{p}' m_2'' m'_3 \nu_2'' \nu_3' | \varphi_d \rangle}{-|\epsilon_d| - \frac{1}{m}(\mathbf{p}^2 + \mathbf{p}'^2 + \mathbf{p} \cdot \mathbf{p}') + \frac{3}{2m}(\mathbf{p} + \mathbf{p}') \cdot \mathbf{q}_0 + i\epsilon}. \tag{B4}$$

For the extraction of the asymptotic limit as $\frac{3}{4}|\mathbf{q}_0| \rightarrow \infty$ we refer to a previous study [6] carried out for 3 bosons. We use Eq. (A5) and use the deuteron wave function given in configuration space. After some algebra one arrives at

$$\begin{aligned}
\hat{I} \longrightarrow & -\frac{i}{3q_0} m 2\pi^2 (-)^{\frac{1}{2}-\nu_3} (-)^{\frac{1}{2}-\nu'_2} \delta_{\nu_1, -\nu_3} \delta_{\nu'_3, -\nu'_2} \\
& \times \sum_l C(l11, 0m_d) \left(\frac{1}{2} \frac{1}{2} 1, m_3 m_d - m_3\right) \sqrt{2l+1} \\
& \times \sum_{l'} C(l'11, 0m_d) \left(\frac{1}{2} \frac{1}{2} 1, m'_2 m_d - m'_2\right) \sqrt{2l'+1} \\
& \times i^{l'-l} \int_0^\infty dr \varphi_l(r) \varphi_{l'}(r) \delta_{m_1, m_d - m_3} \delta_{m'_3, m_d - m'_2}. \tag{B5}
\end{aligned}$$

The second term in Eq. (2.17) can be evaluated analogously and we end up with the intermediate result

$$\begin{aligned}
\langle \Phi | P(t - t^\dagger) P G_0 t P | \Phi \rangle = & -\frac{2im}{3q_0} (2\pi)^2 \sum_{m_3 \nu_3} \sum_{m'_2 \nu'_2} \sum_{m''_2 \nu''_2} \\
& \langle \frac{3}{4} \mathbf{q}_0 m_2^0 m_3 \nu_2^0 \nu_3 | t - t^\dagger | \frac{3}{4} \mathbf{q}_0 m'_2 m_d - m''_2, \nu'_2, -\nu''_2 \rangle_{na} \\
& \langle -\frac{3}{4} \mathbf{q}_0 m_d - m_3, m'_2, -\nu_3, \nu_2 | t | \frac{3}{4} \mathbf{q}_0 m_1^0 m_2'' \nu_1^0 \nu_2'' \rangle_{na} (-)^{\frac{1}{2}-\nu_3} (-)^{\frac{1}{2}-\nu''_2} \\
& \sum_l \sqrt{2l+1} C(l11, 0m_d) \left(\frac{1}{2} \frac{1}{2} 1, m_3 m_d - m_3\right) \\
& \sum_{l'} \sqrt{2l'+1} C(l'11, 0m_d) \left(\frac{1}{2} \frac{1}{2} 1, m''_2 m_d - m''_2\right) \\
& i^{l'-l} \int_0^\infty dr \varphi_{l'}(r) \varphi_l(r). \tag{B6}
\end{aligned}$$

We encounter only forward or backward NN scattering amplitudes, which induces connections between the magnetic spin quantum numbers occurring in the t-matrices (put $\hat{q}_0 = \mathbf{z}$). Further we sum over the initial spin magnetic quantum numbers m_d and m_N . As an example of these summations we show the result

$$\begin{aligned}
& \sum_{m_N m_d} \{ \langle \Phi | P(t - t^\dagger) P G_0 t P | \Phi \rangle - \text{complex conjugate} \} = \\
& i \frac{3q_0}{2m} \frac{1}{2\pi^4} \sum_l \sqrt{2l+1} \sum_{l'} \sqrt{2l'+1} i^{l'-l} \int_0^\infty dr \varphi_l(r) \varphi_{l'}(r)
\end{aligned}$$

$$\begin{aligned}
& \left[2C(l11, 01)C(l'11, 01) \left\{ \sigma_{NN}^{tot} \left(\frac{1}{2} \frac{1}{2} np \right) + \sigma_{NN}^{tot} \left(\frac{1}{2} \frac{1}{2} nn \right) + \sigma_{NN}^{tot} \left(\frac{1}{2} - \frac{1}{2} np \right) \sigma_{NN}^{tot} \left(\frac{1}{2} - \frac{1}{2} nn \right) \right\} \right. \\
& \left. + C(l11, 00)C(l'11, 00) \left\{ \sigma_{NN}^{tot} \left(\frac{1}{2} \frac{1}{2} np \right) \sigma_{NN}^{tot} \left(\frac{1}{2} - \frac{1}{2} nn \right) + \sigma_{NN}^{tot} \left(\frac{1}{2} - \frac{1}{2} np \right) \sigma_{NN}^{tot} \left(\frac{1}{2} \frac{1}{2} nn \right) \right\} \right] \\
& - i \frac{8m}{3q_0} (2\pi)^2 \sum_l \sqrt{2l+1} \sum_{l'} \sqrt{2l'+1} i^{l'-l} \int_0^\infty dr \varphi_l(r) \varphi_{l'}(r) \\
& \left[2C(l11, 01)C(l'11, 01) \right. \\
& \left. \{ (Im < \frac{3}{4} \mathbf{q}_0 \frac{1}{2} \frac{1}{2} np | t | \frac{3}{4} \mathbf{q}_0 \frac{1}{2} \frac{1}{2} pn >_{na})^2 + (Im < \frac{3}{4} \mathbf{q}_0 \frac{1}{2} - \frac{1}{2} np | t | \frac{3}{4} \mathbf{q}_0 \frac{1}{2} - \frac{1}{2} pn >_{na})^2 \} \right. \\
& \left. + C(l11, 00)C(l'11, 00) \right. \\
& \left. \{ 2(Im < \frac{3}{4} \mathbf{q}_0 \frac{1}{2} \frac{1}{2} np | t | \frac{3}{4} \mathbf{q}_0 \frac{1}{2} \frac{1}{2} pn >_{na}) (Im < \frac{3}{4} \mathbf{q}_0 \frac{1}{2} - \frac{1}{2} pn | t | \frac{3}{4} \mathbf{q}_0 \frac{1}{2} - \frac{1}{2} np >_{na}) \right. \\
& \left. + (Im < \frac{3}{4} \mathbf{q}_0 \frac{1}{2} - \frac{1}{2} np | t | - \frac{3}{4} \mathbf{q}_0 \frac{1}{2} \frac{1}{2} pn >_{na})^2 \right. \\
& \left. - 2(Im < \frac{3}{4} \mathbf{q}_0 \frac{1}{2} - \frac{1}{2} np | t | - \frac{3}{4} \mathbf{q}_0 \frac{1}{2} \frac{1}{2} np >_{na}) (Im < \frac{3}{4} \mathbf{q}_0 \frac{1}{2} - \frac{1}{2} nn | t | - \frac{3}{4} \mathbf{q}_0 \frac{1}{2} \frac{1}{2} nn >_{na}) \right\}. \tag{B7}
\end{aligned}$$

The last term in Eq. (2.7) can be treated analogously to Eq.(B1) resulting in

$$\begin{aligned}
\langle \Phi | P t^\dagger P (G_0 - G_0^*) t P | \Phi \rangle & \rightarrow -8\pi i \sum_{m_1 m_3 \nu_1 \nu_3} \sum_{m_2' m_3' \nu_2' \nu_3'} \sum_{m_2'' \nu_2''} \\
& < \frac{3}{4} \mathbf{q}_0 m_2^0 m_3 \nu_2^0 \nu_3 | t^\dagger | \frac{3}{4} \mathbf{q}_0 m_2' m_3', \nu_2' \nu_3' >_{na} \\
& \times < -\frac{3}{4} \mathbf{q}_0 m_1 m_2' \nu_1 \nu_2' | t | \frac{3}{4} \mathbf{q}_0 m_1'' m_2'' \nu_1'' \nu_2'' >_{na} \tilde{I}, \tag{B8}
\end{aligned}$$

where

$$\begin{aligned}
\tilde{I} & = \int d^3 p \int d^3 p' < \varphi_d | - \mathbf{p} m_3 m_1 \nu_3 \nu_1 > < - \mathbf{p}' m_2' m_3' \nu_2' \nu_3' | \varphi_d > \\
& \delta(-|\epsilon_d| - \frac{1}{m} (\mathbf{p}^2 + \mathbf{p}'^2 + \mathbf{p}' \cdot \mathbf{p}) + \frac{3}{2m} \mathbf{q}_0 \cdot (\mathbf{p} + \mathbf{p}')).
\end{aligned}$$

It is easily shown that in the high energy limit

$$\tilde{I} = -\frac{1}{i\pi} \hat{I}. \tag{B9}$$

It remains to perform the summations over the spin- and isospin quantum numbers. Then using the connection to the total nd cross section, Eq. (2.4), the lengthy expression Eq. (2.19) results.

TABLES

E_{lab} (MeV)	σ_{nd}^{tot} (mb)				
	$j_{max} = 1$	$j_{max} = 2$	$j_{max} = 3$	$j_{max} = 4$	$j_{max} = 5$
10.0	954.9	1038.0	1035.2	1037.3	1036.7
60.0	141.0	177.8	177.0	177.4	177.3
140.0	43.0	71.6	73.2	74.7	74.6
200.0	31.7	55.8	58.3	60.5	60.4
260.0	29.7	49.4	52.2	54.7	54.7
300.0	29.9	46.9	49.7	52.3	52.4

TABLE I. The convergence of the calculated total nd cross section with increasing j_{max} at selected energies. As NN interaction the CD-Bonn potential has been used.

E_{lab} (MeV)	σ_{nd}^{tot} (mb)			
	AV18	CD-Bonn	NijmI	NijmII
10.0	1039.0	1035.2	1038.0	1038.3
100.0	97.7	99.3	98.2	97.5
140.0	72.2	73.2	72.5	71.8
200.0	57.8	58.3	57.9	57.4
300.0	49.5	49.7	49.6	49.3

TABLE II. Stability of the calculated total nd cross section σ_{nd}^{tot} under the exchange of the NN potentials. The calculations were performed with $j_{max} = 3$.

E_{lab} (MeV)	σ_{nd}^{tot} (mb)							
	Faddeev Calculation				High Energy Expansion			
	full FC	1.ord.	2.ord.	1.+2.ord.	$\sigma_{np} + \sigma_{nn}$	$\sigma_I^{(2)}$	$\sigma_{II}^{(2)}$	sum
100.	100.95	108.27	1.91	110.18	105.60	20.62	-6.54	119.67
140.	74.85	78.62	0.08	78.69	80.23	12.20	-3.96	88.45
200.	60.55	62.74	-0.86	61.89	65.86	6.28	-2.80	69.34
300.	52.30	54.05	-1.52	52.53	58.14	2.38	-2.28	58.24

TABLE III. Comparison of Faddeev results with the asymptotic expansion ones. The calculations were performed throughout with the CD-Bonn potential and $j_{max} = 4$. The terms $\sigma_I^{(2)}$ and $\sigma_{II}^{(2)}$ are from Eq. (2.19). For more explanation of the different terms see Sec. II and III.

FIGURES

FIG. 1. Comparison of the Faddeev calculation for the total nd cross section based on the CD-Bonn [9] potential with data [1]. The experimental values for the total cross section for deuterium were obtained by adding the separately measured values of the hydrogen cross section and the deuterium-hydrogen cross section difference (for details see Ref. [1]). Error bars are omitted, since they are smaller than the dot size.

FIG. 2. The contributions to the total nd cross section of the different orders in the multiple scattering expansion of the Faddeev amplitude. Successive orders are added to the first order term and then compared with the full Faddeev calculation. The potential employed is the CD-Bonn model.

FIG. 3. The contributions of the different orders in the NN t-matrix in the high energy limit to the total nd cross section. The solid line shows the sum of the np and nn total cross sections. The positive contribution $\sigma_I^{(2)}$ (dashed line) drops faster in energy than the negative contribution $\sigma_{II}^{(2)}$ (its magnitude is shown as dotted line) of the second order term of the multiple scattering. For details see Sec. III.

FIG. 4. The contributions to the total nd cross section in the high energy limit. The dashed line shows the sum of the np and nn total cross sections. Successively added to this is the positive contribution $\sigma_I^{(2)}$ (dotted line) and the negative contribution $\sigma_{II}^{(2)}$ (solid line). For details see Sec. III.

FIG. 5. Corrections to the Faddeev calculation based on a nonrelativistic Hamiltonian using strictly two-nucleon forces (solid line) for the total nd cross section. The open squares show calculations at various energies, where the Tucson-Melbourne 3N force has been included. The open triangles show at various energies calculations based on two-nucleon forces corrected with a relativistic kinematic (for details see Sec. IV). The dots describe the data [1]. All calculations are based on the CD-Bonn potential.

Fig.1

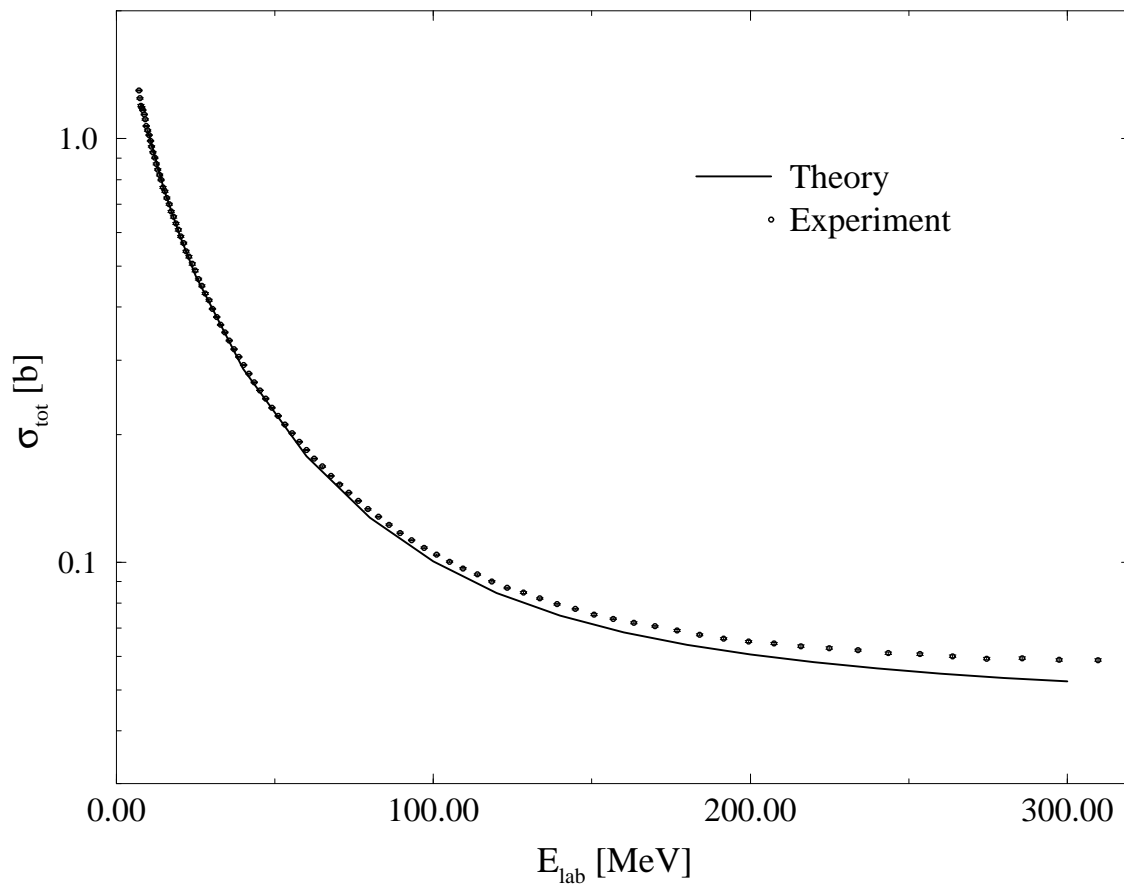


Fig.2

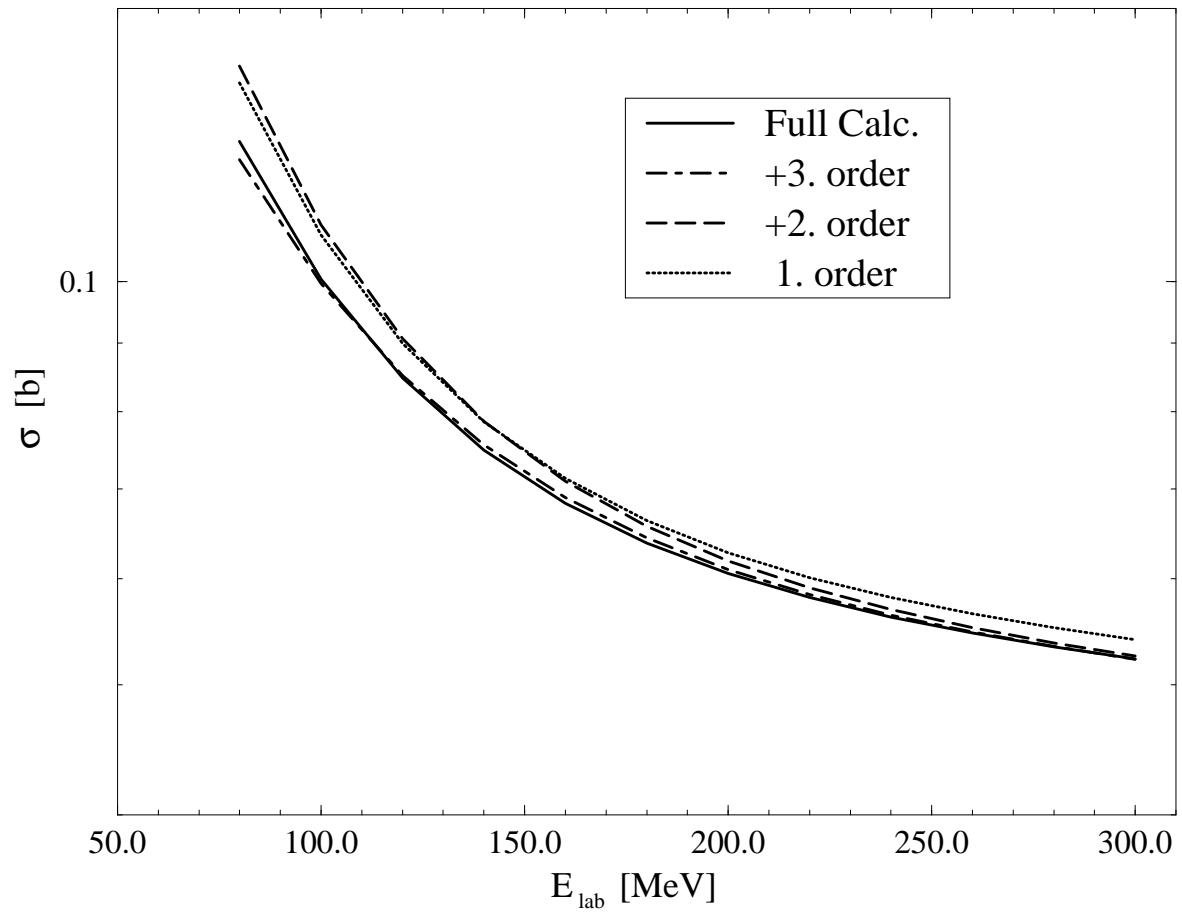


Fig.3

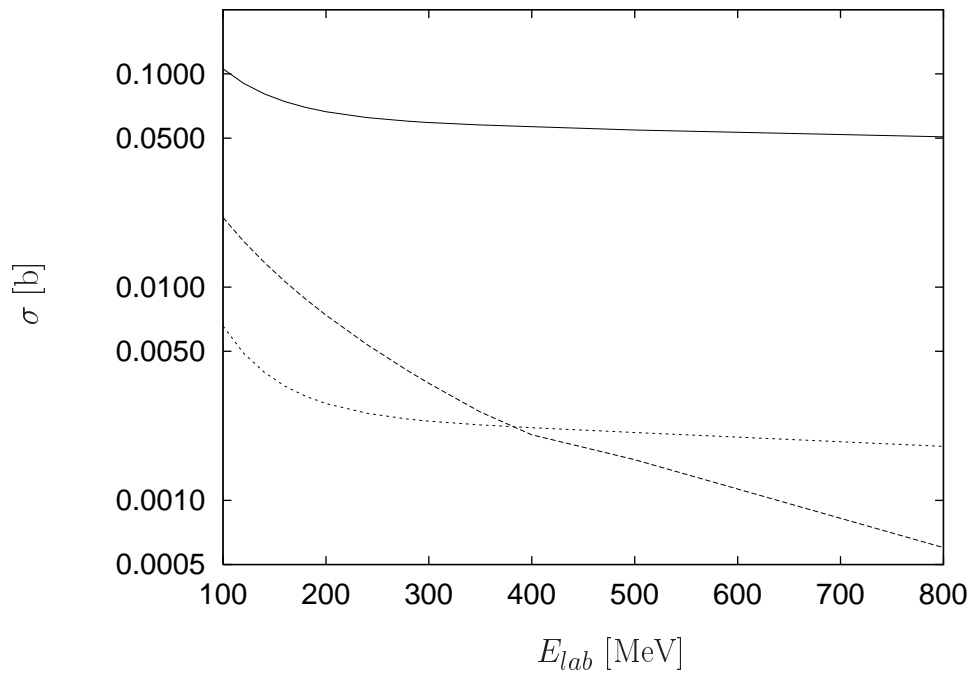


Fig.4

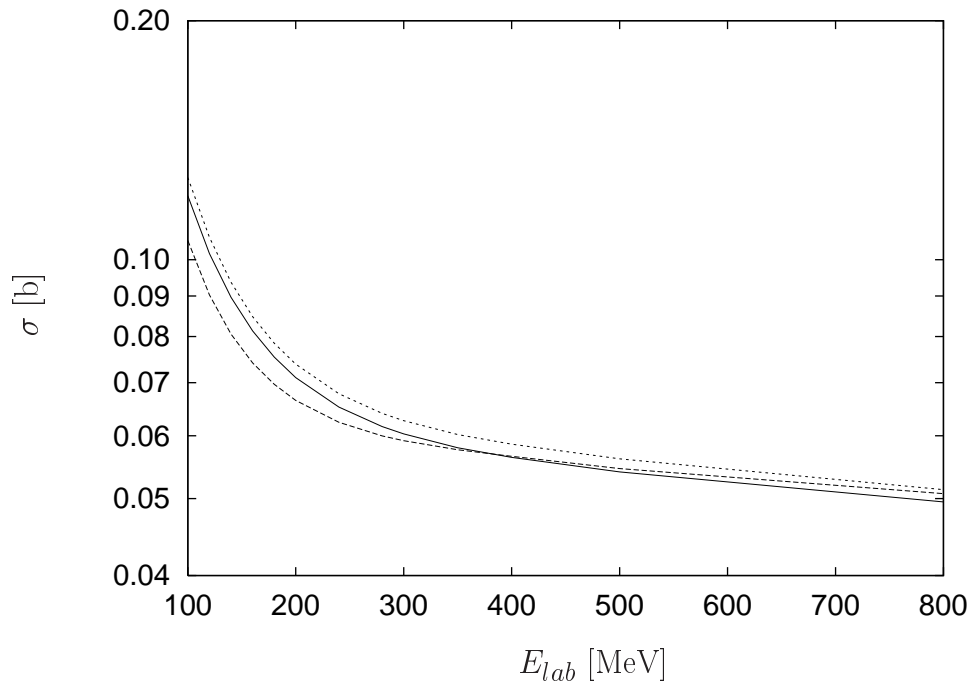


Fig.5

